Free energy of twisting spins in Mn₃Sn

Xiaokang Li , ** Shan Jiang , **, ** Qingkai Meng, ** Huakun Zuo, ** Zengwei Zhu , **, ** Leon Balents , **, ** and Kamran Behnia ** Wuhan National High Magnetic Field Center and School of Physics, Huazhong University of Science and Technology, Wuhan 430074, China

** Laboratoire de Physique et d'Étude des Matériaux (ESPCI - CNRS - Sorbonne Université), PSL Research University, 75005 Paris, France

** Kavli Institute for Theoretical Physics, University of California, Santa Barbara, California 93106-4030, USA

** Canadian Institute for Advanced Research, Toronto, Ontario, Canada



(Received 14 October 2021; revised 28 February 2022; accepted 13 June 2022; published 18 July 2022)

The magnetic free energy is usually quadratic in the magnetic field and depends on the mutual orientation of the magnetic field and the crystalline axes. Tiny in magnitude, this magnetocrystalline anisotropy energy (MAE) is nevertheless indispensable for the existence of permanent magnets. Here, we show that in Mn_3Sn , a noncollinear antiferromagnet that has attracted much attention following the discovery of its large anomalous Hall effect, the free energy of the spins has superquadratic components, which drive the MAE. We experimentally demonstrate that the thermodynamic free energy includes terms odd in the magnetic field $[F(H^3) + F(H^5)]$ and generating sixfold and 12-fold angular oscillations in the torque response. We show that they are quantitatively explained by theory, which can be used to quantify relevant energy scales (Heisenberg, Dzyaloshinskii-Moriya, Zeeman, and single-ion anisotropy) of the system. Based on the theory, we conclude that in contrast to common magnets, what drives the MAE in Mn_3Sn is the field-induced deformation of the spin texture.

DOI: 10.1103/PhysRevB.106.L020402

Aligned spins located on two adjacent atoms are affected by the anisotropic electrostatic forces connecting their orbital angular momenta [1]. This magnetocrystalline anisotropy energy (MAE), a consequence of the spin-orbit coupling, is remarkably small (\sim 60 μ eV/atom in Co and \sim 1 μ eV/atom in Fe and Ni). Since it is the outcome of the competition between energies that are many orders of magnitude larger, it is hard to calculate from first principles [2,3].

Mn₃Sn, a noncollinear antiferromagnet with an inverse triangle spin structure located on a breathing kagome lattice [4], has attracted much attention following the observation of a large anomalous Hall effect (AHE) [5] with a sizable net Berry curvature near the Fermi level [6]. The discovery was followed by the observation of various counterparts of AHE, including the anomalous Nernst [7,8] and the anomalous thermal Hall effects [8-10], as well as the anomalous magneto-optical Kerr effect [11,12]. These are room-temperature effects requiring a small magnetic field. Therefore, Mn₃Sn is potentially attractive in the field of antiferromagnetic spintronics [13–16] or as a Nernst thermopile [7,17]. The peculiar spin texture of Mn₃Sn has been the subject of several studies [18–23]. The magnetic Hamiltonian includes Heisenberg and Dzyaloshinskii-Moriya spin-spin interaction terms dominating by far the small single-ion anisotropy term [19]. A study of torque magnetometry [24] quantified the latter. Previous experiments have documented that magnetic domain walls are chiral [25] and host a topological Hall effect [26].

In this Letter, combining experimental and theoretical study of angular magnetization and torque magnetometry, we have resolved different components (up to the fifth order) of magnetic free energy in a kagome antiferromagnet Mn₃Sn, including two rare odd terms with superquadratic field dependence and presenting sixfold and 12-fold oscillations. Moreover, the quantitative agreement between theory and torque magnetometry experiments permits us to quantify all relevant energy scales of spin interactions such as Heisenberg, Dzyaloshinskii-Moriya, Zeeman, and single-ion anisotropy.

Figure 1 shows in-plane, M_{ab} , and out-of-plane, M_c , magnetization. As shown in Figs. 1(b)–1(e), after subtracting the linear background, we find an additional term that is quadratic in the magnetic field. We conclude that the magnetization consists of at least three terms:

$$M_{\text{total}} = M_0 + M_1 + M_2 + O(H^3) \approx m_0 + \chi H + CH^2$$
. (1)

The first two terms are the zero-field spontaneous weak ferromagnetism and the linear paramagnetism, respectively, resolved in previous studies [5]. The third term, M_2 , was not detected in previous studies and represents a second-order correction to the magnetization response [27–30]. Since the magnetization is the partial derivative of the magnetic free energy with respect to the magnetic field $(M = \partial F_M/\partial H)$, a finite M_2 implies an additional term for the magnetic free energy.

$$F_M = \sum_i m_{0,i} H_i + \frac{1}{2} \sum_{i,j} \chi_{i,j} H_i H_j + \frac{1}{3} \sum_{i,j,k} C_{i,j,k} H_i H_j H_k.$$
(2)

Here, $C_{i,j,k}$ is a 3 × 3 × 3 tensor, which represents the second odd term in the field dependence of the free energy.

^{*}lixiaokang@hust.edu.cn

[†]zengwei.zhu@hust.edu.cn

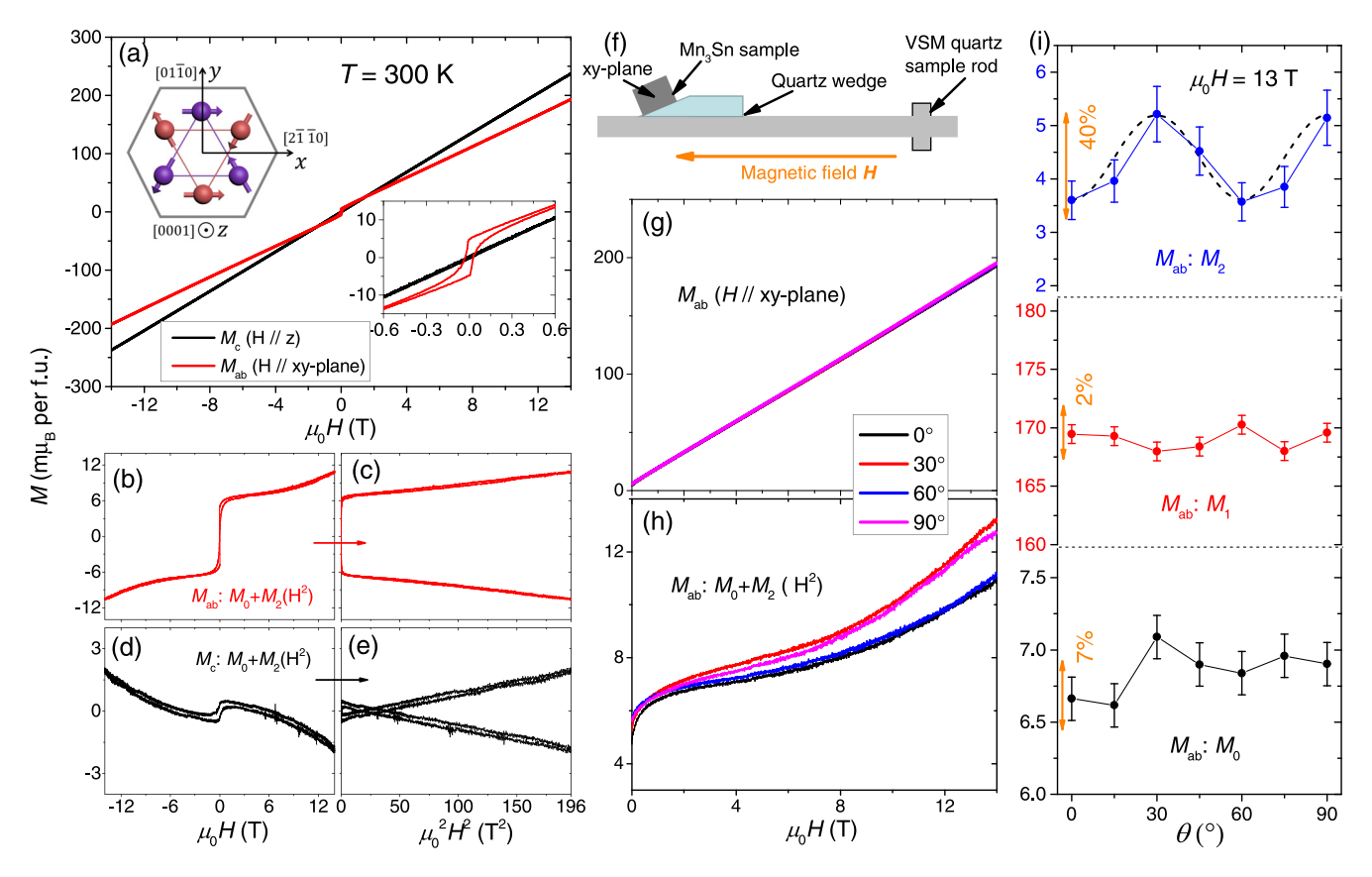


FIG. 1. A quadratic term in the magnetization of Mn_3Sn : (a) In-plane, M_{ab} , and out-of-plane, M_c , magnetization in Mn_3Sn at 300 K; the insets show the zoom-in and the spin texture, respectively. (b), (c) The residual component of M_{ab} after subtracting its dominant linear term $M_1(\propto O(H))$. It is plotted with the (b) linear and (c) quadratic x coordinate, respectively. (d), (e) The residual component of M_c . (f) Experimental configuration for the angular magnetization. (g), (h) Comparison of M_{ab} and its residual component with four different angles: 0° , 30° , 60° , and 90° , respectively. (i) The angle dependence of the M_0 , M_1 , and M_2 . Only the latter show angular oscillations with a periodicity of 60 degrees.

The angular variation of these three terms was investigated by measuring magnetization at different angles, using the setup shown in Fig. 1(f). Rotation was achieved by changing the sharp angle of a quartz wedge held between the sample and the sample holder. Figures 1(g) and 1(h) show magnetization and its residual after subtracting the linear background as a function of field for four different angles in the ab plane.

The angle dependence of in-plane M_0 , M_1 , and M_2 is plotted in Fig. 1(i). In contrast to M_0 and M_1 , M_2 displays a clear sixfold symmetry. We conclude that $F^3(H^3)$ has a sixfold anisotropic component and $M_2 = M_{2,0} + M_{2,6} \cos(6\phi)$. At 13 T, $M_{2,0} = 4.4 \, m\mu_B/\text{f.u.}$ and $M_{2,6} = 0.8 \, m\mu_B/\text{f.u.}$ As we will see below, the magnitude of the latter term is confirmed with a higher precision by measurements of the magnetic torque τ , which quantifies the angular derivative of the magnetic free energy ($\tau = \partial F_M/\partial\theta$).

Figure 2(a) shows the torque setup. The applied magnetic field rotates in the ab plane of the sample, and the magnetic torque along the c axis is detected by the variation in the capacitance between two metal plates. Figure 2(b) shows the angular dependence of the torque signal below 6 T resolving a clear sixfold symmetry. However, a deviation becomes visible at higher magnetic field. As seen in Fig. 2(c), when the magnetic field increases from 6 to 13 T, the shape of each oscillation, instead of being sinelike, becomes sawtoothlike.

This is caused by the emergence of an additional angledependent term.

In addition to the twofold and sixfold terms detected before [24], our data has an additional term with 12-fold symmetry. Figures 2(d)-2(f) show the difference between the data and the sum of the two first terms $(K_2 \sin[2(\theta + \phi_2)] + K_6 \sin[6(\theta + \phi_6)])$; the residual has a clear 12-fold anisotropy $(K_{12} \sin[12(\theta + \phi_{12})])$. The evolution of the fitting parameters K_2 , K_6 , and K_{12} with the magnetic field is shown in Fig. 2(g). $K_2(H)$ follows $H^{3/2}$. $K_6(H)$ remains the largest term in the whole field range. Its field dependence approximately follows H^3 . $K_{12}(H)$ shows the steepest field dependence and is close to H^5 at low fields.

The strong field dependence of the torque components of Mn_3Sn is in sharp contrast with what is seen in ferromagnets [31], as confirmed by our own data on bcc Fe (see the Supplemental Material (SM) [32]). The twofold term K_2 evolves much slower than H^3 and strongly depends on the sample aspect ratio (see the SM [32]), implying its extrinsic origin, such as the shape anisotropy.

The sixfold term K_6 shows a field dependence clearly linking it to the field-cubic free energy $[F^3(H^3)]$, confirming what was deduced from measurements of angle-dependent magnetization. Both sets of data lead to the conclusion that there is a component of free energy with sixfold angular

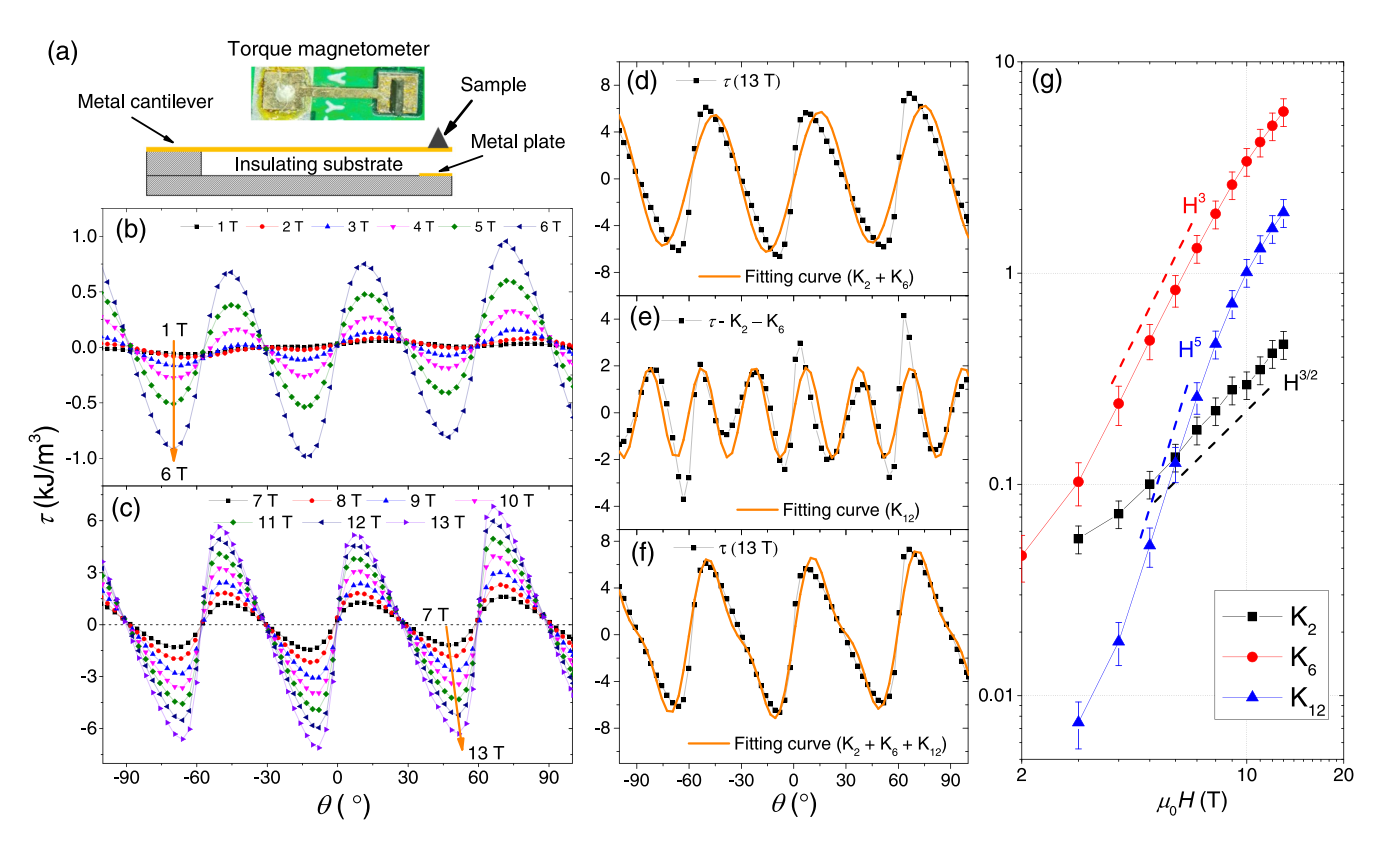


FIG. 2. Magnetic torque measurements. (a) The homemade experimental setup and its photograph (top) with a capacitive torque magnetometer, rotating the field in the xy plane of the Mn₃Sn sample. (b) The angle-dependent torque responses for magnetic fields up to 6 T. (c) The angle-dependent torque responses for magnetic fields larger than 6 T. $H \parallel x$ corresponds to 0° . (d) Fit to the 13 T data with an expression that has only a twofold and a sixfold term $(\tau = K_2 \sin[2(\phi + \phi_2)] + K_6 \sin[6(\phi + \phi_6)])$. The mismatch is obvious. (e) The residual torque component after subtracting the data and the previous fit. It shows a clear 12-fold symmetry. (f) A fit which includes an additional 12-fold symmetry component $(K_{12} \sin[12(\phi + \phi_{12})])$. (g) Fitting parameters $K_2(H)$, $K_6(H)$, and $K_{12}(H)$ as a function of magnetic field.

symmetry and cubic field dependence $(F^{(3,6)} \propto H^3 \cos 6\theta)$. A consistency check can be done by comparing the magnitude of K_6 , the angle derivative, and $M_{2,6}$, the field derivative. At 13 T, K_6 is 4700–5600 Jm⁻³, implying $F^{(3,6)} \approx 0.34 \pm 4 \, \mu \text{eV}/\text{f.u.}$, and $M_{2,6}$ is $0.8 \, m \mu_B$ per f.u., corresponding to $F^{(3,6)} \approx 0.20 \, \mu \text{eV}/\text{f.u.}$. The difference may result from the low-order $(<H^3)$ contribution of K_6 . The list of all components of the free energy identified by our experiments is given in Table I. Let us now show that theory provides a satisfactory account of the existence and the amplitude of the K_6 term as well as the emergence and rapid growth of the secondary K_{12} term with increasing magnetic field.

Following Liu and Balents [19], the energy per magnetic unit cell (six spins) consists of the sum of four terms [see Fig. 3(b)] (see the SM [32]), written in terms of spin vectors S_i on the three sublattices i = 1, 2, 3 (with $4 \leftrightarrow 1$ identified). These are as follows: Heisenberg,

 $4J\sum_{i}S_{i}\cdot S_{i+1}$; Dzyaloshinskii-Moriya (DM), $4D\sum_{i}\hat{z}\cdot S_{i}\times S_{i+1}$; single-ion-anisotropy (SIA), $-2K\sum_{i}(S_{i}\cdot\hat{e}_{i})^{2}$; and Zeeman, $-2\mu\sum_{i}H\cdot S_{i}$. For D>0 and in the absence of SIA and Zeeman terms, the ground state is an antichiral state with in-plane spins. A finite magnetic field will distort the spin triangles [see Fig. 3(a)] by some small amounts η_{i} from the ideal 120° state. The distortion angles η_{i} are small because, in our window of investigation (H<14 T), one has $K\ll J$ and $\mu H\ll J$. In the Supplemental Material [32], we extend the treatment in Ref. [8] to obtain a perturbative expansion for the free energy and angles in the small parameters K/J, $\mu H/J\ll 1$, which are indeed small in our experimental window (H<14 T). This leads to an expression for the free energy per unit cell (see the SM [32]).

The first term is linear in the magnetic field,

$$F^{(1,ab)} = \frac{K\mu H}{J + \sqrt{3}D}. (3)$$

TABLE I. Components of the magnetic free energy in Mn_3Sn identified by measurements of magnetization (M_0 , M_1 , and M_2) and torque (K_2 , K_6 , and K_{12}). Experimental amplitudes refer to what was measured at 13 T, expressed in units of μ eV/Mn.

Component	$F^{(1,ab)}$	$F^{(1,c)}$	$F^{(2,ab)}$	$F^{(2,c)}$	$F^{(3,0)}$	$F^{(3,6)}$	$F^{(5,12)}$	$F^{(1.5,2)}$
Experimental responses	M_0^{ab}	M_0^c	$m{M}_1^{ab}$	M_1^c	$M_{2,0}^{ab}$	$M_{2.6}^{ab}/K_6$	K_{12}	K_2
Experimental amplitude	1.7	0.11	21.4	27.9	0.37	0.067/0.115	0.018	0.028

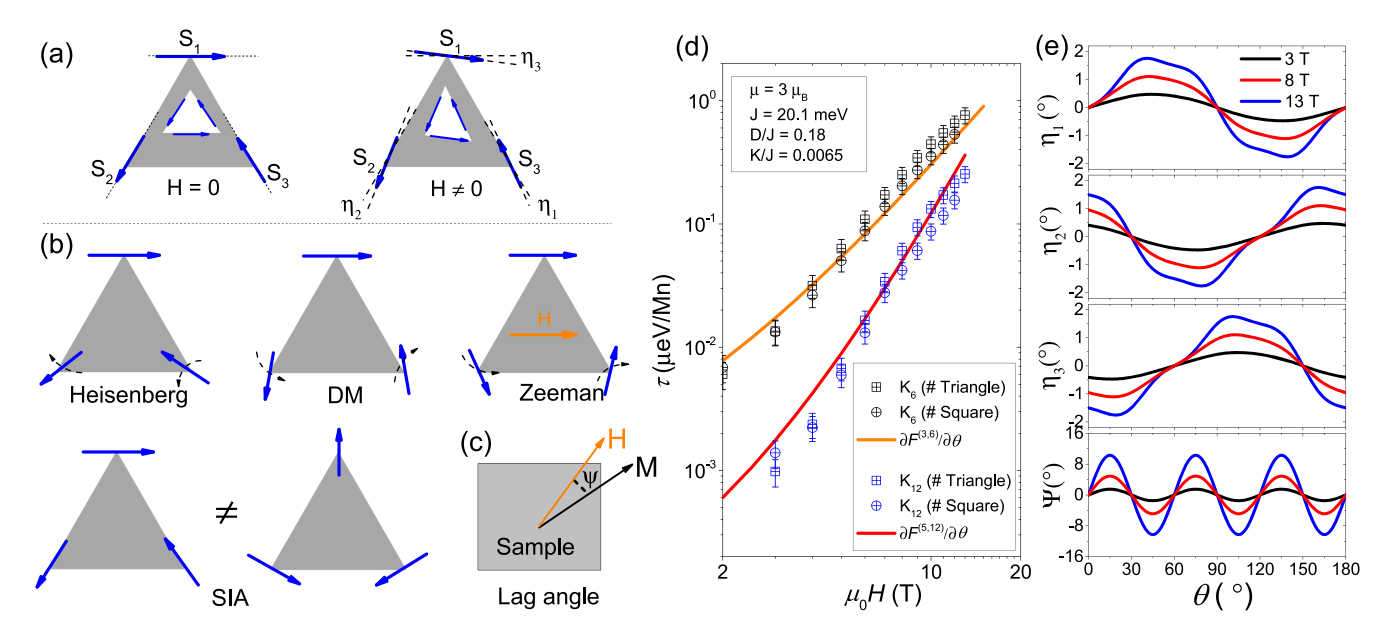


FIG. 3. Magnetocrystalline anisotropy driven by field-induced twist of nonaligned spins. (a) The magnetic field distorts the spin triangle (in white), which is no longer isomorphic to the lattice triangle (in gray). The deformation angles η_i quantify the distortion. (b) The interaction between one spin and its immediate neighbors favors clockwise and anticlockwise twists. The Zeeman effect favors alignment of all spins with the magnetic field. Single-ion anisotropy causes inequivalency between the two perpendicular orientations of the spin triangle with respect to the lattice triangle. (c) The lag angle ψ between the rotated magnetic field and the total magnetization. (d) The experimental K_6 and K_{12} (symbols) compared to theoretical expectation (solid line) using $\mu = 3\mu_B$, J = 20.1 meV, D/J = 0.18, K/J = 0.0065. (e) The deformation angles η_i and lag angle ψ at 3, 8, and 13 T predicted by theory (see the SM [32]).

The quadratic term (see the SM [32]) has slightly different expressions for in-plane and out-of-plane orientations of the magnetic field,

$$F^{(2,ab)} = \frac{(\mu H)^2}{2J} \left(1 - \frac{\sqrt{3}D}{J} \right),$$

$$F^{(2,c)} = \frac{(\mu H)^2}{2J} \left(1 - \frac{D}{\sqrt{3}J} \right).$$
 (4)

Therefore, one expects the quadratic free energy to be larger for the out-of-plane orientation of the magnetic field, in agreement with what is seen experimentally (see Table I). For the in-plane configuration, the first correction to the quadratic term has a $\cos 6\theta$ angle dependence. Its amplitude is equal to

$$F^{(3,6)} = \frac{(K + \mu H)^2 [(3J + 7\sqrt{3}D)K + 4\sqrt{3}D\mu H]}{36(J + \sqrt{3}D)^3}.$$
 (5)

The term with highest exponent is H^3 . As one can see in Fig. 3(d), this expression provides an excellent account of the field and angular dependence of the experimentally observed K_6 . The next component has a $\sin^2(6\theta)$ angle dependence and is equal to

$$F^{(5,12)} = \frac{(K + \mu H)^2}{72(J + \sqrt{3}D)^5 \mu H K} [(3J + 7\sqrt{3}D)K^2 + 2(J + 4\sqrt{3}D)\mu H K + 2\sqrt{3}D(\mu H)^2]^2.$$
 (6)

Here, the highest-order term is H^5 and it accounts for the emergence of K_{12} in the torque data and its field dependence [see Fig. 3(d)]. The model also yields the evolution of the deformation angles η_i and the lag angle ψ with the rotating magnetic field. They are plotted in Fig. 3(e).

The agreement between theory and experiment allows us to extract the energy scales of the system. Taking the magnetic moment of each Mn atom to be $\mu = 3 \mu_B$, as reported by neutron diffraction studies [33,34], we extracted J, D, and K by fitting the torque data with the angle derivative $F^{(3,6)}$ and $F^{(5,12)}$, as seen in Fig. 3(d). The results are summarized in Table II. Alternatively, one can use the magnetization data and the field derivatives $F^{(1,ab)}$, $F^{(2,ab)}$, and $F^{(2,c)}$; the results are given in the second row of Table II. As seen in Table II, J = 20.1 meV, which is somewhat larger than what is yielded by magnetization. There are several plausible sources for this. One is the presence of additional ferromagnetic couplings between spins of the same sublattice [21], which enhance the magnetization but do not contribute to torque. A second is field-induced out-of-plane spin canting [26] neglected in the present model. A third possible source is a finite orbital contribution [35–39] to the in-plane magnetization (see the SM for details [32]). We note that our result for J is fairly close to the what has been reported by a study of magnon dispersion by inelastic neutron scattering (18 meV) [21]. Finally, our study pins down the values for K and D.

TABLE II. The energy scales of Mn_3Sn extracted from the torque and magnetization data using the theoretical expressions of the free energy.

Parameter	J (meV)	D/J	K/J	
Torque	20.1(8)	0.18(2)	0.0065(5)	
Magnetization	13.8	0.18	0.0058	

In summary, the magnetic free energy in Mn₃Sn includes odd terms with superquadratic field dependence and presenting sixfold and 12-fold angular oscillations. Theory invoking a field-induced twist in the orientation of in-plane spins can successfully explain the presence of these terms and their amplitude can be used to extract all energy scales of the system. Our model makes quantitative predictions about the deformation of the spin texture by the magnetic field, which can be checked by future neutron scattering studies. Beyond the specific case of Mn₃Sn, our experiment demonstrates the capacity of torque magnetometry to quantify anisotropic higher-order terms of the magnetic free energy. This may be employed in a variety of magnetic systems, including frustrated magnets and spin-liquid candidates.

This work was supported by the National Science Foundation of China (Grants No. 12004123, No. 51861135104 and No. 11574097), the National Key Research and Development Program of China (Grant No. 2016YFA0401704), the Fundamental Research Funds for the Central Universities (Grant No. 2019kfyXMBZ071). K.B. was supported by the Agence Nationale de la Recherche (Grants No. ANR-18-CE92-0020-01 and No. ANR-19-CE30-0014-04). S.J. acknowledges a Ph.D. scholarship by the China Scholarship Council (CSC). X.L. acknowledges the China National Postdoctoral Program for Innovative Talents (Grant No. BX20200143) and the China Postdoctoral Science Foundation (Grant No. 2020M682386). L.B. was supported by the NSF CMMT program under Grant No. DMR-2116515.

- [1] J. H. van Vleck, Phys. Rev. 52, 1178 (1937).
- [2] G. H. O. Daalderop, P. J. Kelly, and M. F. H. Schuurmans, Phys. Rev. B 41, 11919 (1990).
- [3] S. V. Halilov, A. Y. Perlov, P. M. Oppeneer, A. N. Yaresko, and V. N. Antonov, Phys. Rev. B 57, 9557 (1998).
- [4] S. Tomiyoshi and Y. Yamaguchi, J. Phys. Soc. Jpn. 51, 2478 (1982).
- [5] S. Nakatsuji, N. Kiyohara, and T. Higo, Nature (London) 527, 212 (2015).
- [6] H. Yang, Y. Sun, Y. Zhang, W.-J. Shi, S. S. Parkin, and B. Yan, New J. Phys. 19, 015008 (2017).
- [7] M. Ikhlas et al., Nat. Phys. 13, 1085 (2017).
- [8] X. Li, L. Xu, L. Ding, J. Wang, M. Shen, X. Lu, Z. Zhu, and K. Behnia, Phys. Rev. Lett. 119, 056601 (2017).
- [9] K. Sugii et al., arXiv:1902.06601.
- [10] L. Xu et al., Sci. Adv. 6, eaaz3522 (2020).
- [11] T. Higo et al., Nat. Photon. 12, 73 (2018).
- [12] A. L. Balk et al., Appl. Phys. Lett. 114, 032401 (2019).
- [13] L. Šmejkal, Y. Mokrousov, B. Yan, and A. H. MacDonald, Nat. Phys. 14, 242 (2018).
- [14] V. Baltz, A. Manchon, M. Tsoi, T. Moriyama, T. Ono, and Y. Tserkovnyak, Rev. Mod. Phys. 90, 015005 (2018).
- [15] M. Kimata et al., Nature (London) 565, 627 (2019).
- [16] H. Tsai et al., Nature (London) 580, 608 (2020).
- [17] X. Li, Z. Zhu, and K. Behnia, Adv. Mater. 33, 2100751 (2021).
- [18] J. W. Cable, N. Wakabayashi, and P. Radhakrishna, Phys. Rev. B 48, 6159 (1993).
- [19] J. Liu and L. Balents, Phys. Rev. Lett. 119, 087202 (2017).
- [20] M.-T. Suzuki, T. Koretsune, M. Ochi, and R. Arita, Phys. Rev. B 95, 094406 (2017).
- [21] P. Park et al., npj Quantum Mater. 3, 63 (2018).
- [22] A. Zelenskiy, T. L. Monchesky, M. L. Plumer, and B. W. Southern, Phys. Rev. B 103, 144401 (2021).

- [23] S. Miwa et al., Small Sci. 1, 2000062 (2021).
- [24] T. Duan, W. Ren, W. Liu, S. Li, W. Liu, and Z. Zhang, Appl. Phys. Lett. 107, 082403 (2015).
- [25] X. Li et al., Nat. Commun. 10, 3021 (2019).
- [26] X. Li, L. Xu, H. Zuo, A. Subedi, Z. Zhu, and K. Behnia, SciPost Phys. 5, 063 (2018).
- [27] D. Treves, Phys. Rev. 125, 1843 (1962).
- [28] G. Gorodetsky and D. Treves, Phys. Rev. 135, A97 (1964).
- [29] N. Kharchenko, R. Szymczak, and M. Baran, J. Magn. Magn. Mater. 140–144, 161 (1995).
- [30] T. Liang, T. H. Hsieh, J. J. Ishikawa, S. Nakatsuji, L. Fu, and N. Ong, Nat. Phys. 13, 599 (2017).
- [31] C. D. Graham, Phys. Rev. 112, 1117 (1958).
- [32] See Supplemental Material at http://link.aps.org/supplemental/ 10.1103/PhysRevB.106.L020402 for the sample growth, the measurement method, the reproducibility of data, the magnetization and magnetic torque in bcc iron, the theory of energy from microscopic spin model, and the origin of different estimates of J.
- [33] P. Brown, V. Nunez, F. Tasset, J. Forsyth, and P. Radhakrishna, J. Phys.: Condens. Matter 2, 9409 (1990).
- [34] S. Tomiyoshi, J. Phys. Soc. Jpn. 51, 803 (1982).
- [35] L. M. Sandratskii and J. Kübler, Phys. Rev. Lett. 76, 4963 (1996).
- [36] Y. Chen, J. Gaudet, S. Dasgupta, G. G. Marcus, J. Lin, T. Chen, T. Tomita, M. Ikhlas, Y. Zhao, W. C. Chen, M. B. Stone, O. Tchernyshyov, S. Nakatsuji, and C. Broholm, Phys. Rev. B 102, 054403 (2020).
- [37] J. M. Taylor, A. Markou, E. Lesne, P. K. Sivakumar, C. Luo, F. Radu, P. Werner, C. Felser, and S. S. P. Parkin, Phys. Rev. B 101, 094404 (2020).
- [38] S. Sakamoto, T. Higo, M. Shiga, K. Amemiya, S. Nakatsuji, and S. Miwa, Phys. Rev. B **104**, 134431 (2021).
- [39] M. Kimata et al., Nat. Commun. 12, 5582 (2021).